[7]D. S. Gaunt and C. Domb, J. Phys. C 1, 1038 (1968).
[8]C. S. Koonce, B. W. Mangum, and D. D. Thornton, in *Proceedings of the Twelfth International Conference on Low Temperature Physics*, edited by E. Kanda (Keigaku, Tokyo, 1971).
[9]R. W. G. Wycoff, *Crystal Structures*, 2nd ed. (Interscience, New York, 1965), Chap. VIII.
[10]K. Motizuki, J. Phys. Soc. Japan 14, 759 (1959).
[11]J. Kanamori, Progr. Theoret. Phys. (Kyoto) 20, 890 (1958).
[12]C. J. Gorter and T. Van Peski-Tinbergen, Physica 22, 273 (1956).
[13]M. Ball, W. P. Wolf, and A. F. G. Wyatt, Phys. Letters 10, 7 (1964).
[14]H. W. Capel, Physica 31, 1152 (1965).
[15]B. E. Keen, D. P. Landau, B. Schneider, and W. P. Wolf, J. Appl. Phys. 37, 1120 (1966).
[16]B. E. Keen, D. P. Landau, and W. P. Wolf, Phys. Letters 23, 202 (1966).
[17]W. P. Wolf, in *Critical Phenomena*, edited by M. S. Green and J. V. Sengers, Natl. Bur. Std. (U.S.) Misc. Publ. 273 (U.S. GPO, Washington, D. C., 1965), p. 49.
[18]R. Bidaux and B. Vivet, J. Phys. 29, 57 (1968).
[19]R. Bidaux, P. Carrara, and B. Vivet, J. Phys. 29, 357 (1968).
[20]I. S. Jacobs and P. E. Lawrence, Phys. Rev. 164, 866 (1967).
[21]V. A. Schmidt and S. A. Friedberg, Phys. Rev. B 1, 2250 (1970).
[22]D. P. Landau, B. E. Keen, B. Schneider, and W. P. Wolf, Phys. Rev. B 3, 2310 (1971).
[23]M. E Fisher, Proc. Roy. Soc. (London) A254, 66 (1960).
[24]P. W. Kasteleijn, Physica 22, 387 (1956).
[25]B. R. Heap, Proc. Phys. Soc. (London) 80, 248 (1962).
[26]S. Yomosa, J. Phys. Soc. Japan 15, 1068 (1960).
[27]R. S. Feigelson, J. Am. Ceram. Soc. 47, 257 (1964).
[28]B. W. Mangum and D. D. Thornton, Rev. Sci. Instr. 41, 1764 (1970).
[29]F. G. Brickwedde, H. Van Dijk, M. Durieux, J. R. Clement, and J. K. Logan, Natl. Bur. Std. (U.S.) Monograph No. 10 (U.S. GPO, Washington, D. C., 1960).
[30]Certain commercial equipment, instruments, or materials are identified in this paper in order to adequately specify the experimental procedure. In no case does such identification imply recommendation or endorsement by the National Bureau of Standards, nor does it imply that the material or equipment is necessarily the best available for the purpose.
[31]L. Holmes, R. Sherwood, and L. G. Van Uitert, J. Appl. Phys. 39, 1373 (1968).
[32]P. M. Levy and D. P. Landau, J. Appl. Phys. 39, 1128 (1968).
[33]P. M. Levy, Phys. Rev. 170, 595 (1968).
[34]A. F. G. Wyatt, J. Phys. C 1, 684 (1968).
[35]J. C. Wright (private communication).

PHYSICAL REVIEW B VOLUME 4, NUMBER 11 1 DECEMBER 1971

Measurement of Conduction-Electron Spin-Density Oscillations in Ordered *Fe*Si Alloys

Mary Beth Stearns
Scientific Research Staff, Ford Motor Company, Dearborn, Michigan 48121
(Received 1 February 1971; revised manuscript received 13 May 1971)

Pulsed NMR hyperfine field measurements have been made on ordered $Fe_{1-x}Si_x$ alloys for $0.181 \leq x \leq 0.249$. Using ordered compounds greatly improves the accuracy with which internal-field shifts due to the first nine neighbor shells can be measured. A number of effects which were difficult to observe in dilute alloys are easily measurable. Dipolar structure and saturation or shielding effects are seen for various neighbor shells. We see no damping of the spin density oscillations with alloying. This allows the determination of a lower limit for the mean free path of the conduction electrons in the alloys. The third-, fourth-, and sixth-nearest-neighbor Fe atoms give positive polarizations. The measured hyperfine field shifts are extrapolated and combined with dilute alloy data to obtain the spin-density oscillations surrounding an Fe atom in pure Fe.

I. INTRODUCTION

In metals ferromagnetism is believed to be achieved by the "local" atomic moments being aligned through the intermediary of the polarized "itinerant" electrons.[1] Many experiments and calculations have been carried out in recent years to investigate this interaction. For a discussion of these see the Introduction in the following paper, hereafter referred to as Paper II. The experiments which yield by far the most direct information about the spin density of the itinerant s-like conduction electrons are Mössbauer[2,3] and NMR[4-6] experiments.

A properly chosen system (namely, an alloy system where the solute atom has *no* moment and the form factor of the Fe atoms does not change upon alloying) can give detailed information about the variation of the s-like conduction-electron polarization (CEP) with distance around an Fe atom.

We report on accurate measurements of the hyper-

fine field shifts at Fe and Si atoms due to adding Fe atoms into the first nine shells in ordered alloys near Fe_3Si. The experimental analysis is given in Sec. III. The shifts are interpreted as due to s-like conduction-electron polarization which is closely related to $J_{eff}(\vec{k},\vec{k}')$, the effective exchange interaction between localized and itinerant electrons. The results in these alloys are very similar to those obtained in dilute alloys of FeSi and FeAl,[2] which we feel are representative of CE spin-density oscillations in the pure Fe lattice. Questions on the evaluation and the validity of many assumptions made in the dilute alloy work are directly answerable from this present work. Dipolar effects were measured and are discussed in Sec. IV B. The assumption of additivity which is usually made in dilute alloy work was directly measurable here and is discussed in Sec. IV C. There is no indication of a damping or lessening of the amplitude and phase shift[7] of the spin density oscillation due to disorder caused by going off stoichiometry. This allows a determination of a lower limit of the mean free path for scattering and is discussed in Sec. IV D. From these and the earlier measurements on dilute alloys we are able to obtain a consistent model for the origin of the hyperfine in Fe which incorporates the latest band calculations by Fe.[8] This is discussed in Paper II. Comparison with improved Ruderman-Kittel-Kasuya-Yosida (RKKY) and charge-density oscillation theories is also made in Paper II. From the present measurements we are able to evaluate the hyperfine field contribution due to the Fe neighbors and using this we can understand and explain the observed variation of the hyperfine fields to solute atoms in Fe as presented in Paper II.

The improved resolution we obtain here is largely due to a separation of the effects of the different neighbor shells by the use of an ordered structure. Whereas in dilute alloys each atom feels equally the effects of all shells (e.g., consider the first six) here we have three separate atomic species each of which is sensitive to the effects of only two of these six shells as we go off stoichiometry. This greatly improves the sensitivity. This technique of choosing a stoichiometric ordered compound and varying the composition around stoichiometry is of general applicability and should also be useful in other type experiments, e.g., in NQR experiments which measure the gradient of the charge-density oscillations.

II. EXPERIMENTAL PROCEDURE

Samples of ordered alloys varying from 18.1- to 25-at.% Si (all compositions will be given in at.%) were made in the following manner. A 5-lb ingot of 99.9% purity Fe and high-purity Si was prepared in an induction vacuum furnace. The ingot was then machined to obtain fine turnings which were then ground down to pass through a 74-μ sieve. These powders were next heat treated in an argon atmosphere. They were first heated to 850 °C for about four hours, then slowly cooled to 400 °C and held there overnight. The furnace was then turned off and allowed to cool to room temperature; this took about eight hours. Part of the powdered samples were chemically analyzed to determine the composition. For each alloy two independent chemical analyses were made; they agreed to within 0.1 to 0.2 at.%. Previous Mössbauer experiments[2(a)] have shown that this heat treatment produces essentially perfectly ordered alloys with the excess Fe atoms of the D type (as measured with respect to ordered Fe_3Si) going randomly into the Si sites.

The pulsed NMR apparatus was essentially the same as that described previously.[9] The spectrum of each alloy was taken at 1.2 °K by measuring the echo height as the frequency ν was varied. Before taking the frequency spectrum, the maximum enhancement factor ϵ_m was measured near the center of the spectrum with the technique described in Ref. 9. In another paper being prepared on the variation of ϵ and the relaxation times in these alloys we show that for domain wall motion dominated by damping (due to eddy currents), ϵ_m varies as the $\nu^{1/2}$. However if the stiffness term dominates (e.g., wall surface tension or magnetostatic forces) then ϵ_m varies as $\nu^{3/2}$. These alloys seem to correspond to the case where both these terms are comparable, so ϵ_m varies between the $\frac{1}{2}$ and $\frac{3}{2}$ power of the frequency. This variation is well outside the accuracy of the enhancement factor measurements. For a given type site the maximum change in frequency for a given line is ~2 MHz out of about 40 MHz, so $\Delta\epsilon/\epsilon \sim \frac{1}{20}$, whereas the enhancement factors can only be measured to an accuracy of about 10%.

To obtain meaningful spectra, three conditions should be met. The turning angles, $\alpha = \gamma\epsilon B_1\tau$ (where B_1 is the rf field strength, τ the pulse length, and γ the nuclear gyromagnetic ratio), frequency slice ($\sim \epsilon B_1$), and exciting frequency spectrum ($\sim 1/\tau$) should be kept constant as the frequency is varied. Over frequency intervals large compared with the operating frequency the increase in ϵ (and thus α) should be compensated for by decreasing B_1 so that the frequency slice is constant. However, in these experiments we are only interested in obtaining the variation in intensity for a given type site and do not compare the intensities at different sites. [This was done in the Mössbauer experiments in Ref 2(a).] Thus the frequency interval is only $\sim \frac{1}{20}$ of the operating frequency so these adjustments are negligible. However, in experiments where one is interested in comparing the intensities of different type sites, these considerations become important. Other

effects such as variations of skin depth with frequency may also be important in these cases. Ideally the resolution is improved by taking smaller slices of the frequency spectrum; this means small B_1 values. However there is a proportionate loss in echo intensity as B_1 is decreased. We thus operate at the maximum B_1 which does not lose too much resolution. Further we require that all data for a given type site be taken under the same operating conditions so that the instrumental broadening is constant and we can thus separate out the broadening due to alloying. The linewidths vary from quite narrow lines (for 24.9-at.% Si full width at half-height $\Gamma \sim 150$ kHz ~ 1 kG) to broad lines of $\Gamma \sim 2$ MHz ~ 15 kG. Experimentally we determined that the value of $\tau_1 \simeq 1\,\mu$sec for the first pulse was a good compromise. It showed little loss in resolution or intensity for the spectra of the 23.7-at.% or less Si alloys. The maximum echo signal for a narrow line, $\Gamma << \epsilon B_1$, is obtained when the pulse lengths of the two pulses are in the ratio of 1:2.1 with $\alpha_1 = 5$ rad. We used this pulse ratio. Thus all the spectra were taken with $\tau_1 \simeq 1$ μsec, $\alpha_1 \simeq 5$ rad. This corresponded to B_1 values between 0.15 and 0.6 g depending on the value of ϵ_m (ϵ_m varies between 40 000 and 10 000 for Fe nuclei in these alloys).

The variation of gain with frequency for the overall experimental apparatus was eliminated by simulating the echo on a probe coil (whose resonant frequency was far from the region of measurements) which was loosely coupled to the pickup coil. The simulated pulse had a shape similar to that of the echo. The height of the simulated pulse was then read from the attenuator of the 608D Hewlett Packard oscillator used to produce the simulated pulse. Corrections were made for the variation of output voltage with frequency of the 608D oscillator. A ν^{-1} correction was made for the fact that the signal strength is proportional to the magnetization which varies as $H_{\rm int}$ and thus as the frequency. Since the observed signal is due to the precession of the electrons which are coupled to the nuclei through the enhancement factor ϵ, we should also have another frequency correction factor. At the time of treating the earlier data it was not known how ϵ really varied with frequency so only one factor $1/\nu$ was used. It is now believed that ϵ varies between $\nu^{1/2}$ and $\nu^{3/2}$, so a factor between $\nu^{-3/2}$ and $\nu^{-5/2}$ (say ν^{-2}) should have been used. However for any given spectrum the range of $\Delta\nu$ is small compared with the operating frequency so that the exact variation of ϵ with ν is unimportant. Thus this correction has a negligible effect on the data, so it was not reprocessed with a ν^{-2} correction. The spectra were all taken at 1.2 °K. The repetition rate for a pulse sequence was 400 msec, which is about 20 times longer than the relaxation times at 1.2 °K in these alloys.

III. EXPERIMENTAL RESULTS

The structure of ordered Fe_3Si is shown in Fig. 1. There exist three different type sites; the number and type of neighbors in each shell for each of the sites are listed in Table I. As Fe is added to Fe_3Si the excess atoms go randomly into the Si sites.[2(a)] Since these added Fe atoms always have eight first-nearest-neighbor (1nn) Fe atoms, we will consider them D-type Fe atoms. Thus as we add more Fe we measure the effect of putting D-type Fe atoms in the various shells. Considering the first nine shells only we see that upon deviating from stoichiometry each type site is affected by only three shells rather than the full nine. Since the resonant frequencies for the three sites are well separated (except A_4 and Si), the spectra obtained by going off stoichiometry are thus easily unfolded. Let us now discuss the spectra for each type site.

A. A Sites (1nn, 4nn, 7nn)

From Table I we see that upon increasing the Fe content from Fe_3Si we get some A-type Fe atoms with five or more Fe's in the first-nearest-neighbor shell (1nn) and 13 or more Fe atoms in the 4nn and 7nn shells. We shall denote the A-type atoms by A_m^n where m gives the number of D-type Fe atoms in the 1nn shell and n the number of Fe atoms in the 4nn shell. In the stoichiometric alloy Fe_3Si we have only one A-type line, A_4^{12} at 30.03 ± 0.02 MHz. This is rather close to the Si line at 31.53 ± 0.02 MHz. However a fifth Fe atom in the 1nn shell causes a large frequency shift of 7.2 ± 0.05 MHz, so the A_5^n spectra are well separated from any other lines. Thus the shifts due to adding Fe atoms to the 4nn shells are best obtained from A_5 spectra. For an alloy $Fe_{1-x}Si_x$ the A_m probabilities are given by

$$P_m = \binom{m}{m-4} (4x)^{8-m}(1-4x)^{m-4}, \quad 4 \leq m \leq 8. \quad (1)$$

The fraction P_5^n of each component A_5^n in an alloy of composition $Fe_{1-x}Si_x$ is given by

$$P_5^n = \binom{12}{n-12} (4x)^{24-n}\,(1-4x)^{n-12}, \quad 12 \leq n \leq 24. \quad (2)$$

Figure 2 shows some typical unfolded A_5 spectra. The spectra were unfolded by starting from the right of a spectrum and with the use of a planimeter stripping off the components such that the area of the component A_5^n corresponded to the fraction P_5^n. The widths obtained using this procedure were essentially the same for each component, indicating the model is correct. As x decreases each of the widths of the individual components increases. The broadening of the A_4 and A_5 components as x

TABLE I. Number and type of neighbors for the 3 sites in Fe_3Si. *A* and *D* indicate Fe atoms; the underlines are to emphasize the Si positions.

Type	1nn	2nn	3nn	4nn	5nn	6nn	7nn	8nn	9nn
A-Fe	4*D*-4Si	6*A*	12*A*	12*D*-12Si	8*A*	6*A*	12*D*-12Si	24*A*	24*A*
D-Fe	8*A*	6Si	12*D*	24*A*	8Si	6*D*	24*A*	24Si	24*D*
Si	8*A*	6*D*	12Si	24*A*	8*D*	6Si	24*A*	24*D*	24Si

is decreased allows us to obtain an upper limit to the shift due to the 7nn shell. The procedure for such a determination is discussed in more detail in Sec. II B, in obtaining the shift due to the 5nn shell. From the broadening of the A_4 and A_5 components we found that the shift caused by an Fe atom in the 7nn shell was less than or equal to $|0.2|$ MHz. The relative intensity scales shown for each alloy in Fig. 2 correspond roughly to the A_5 probability calculated from Eq. (1); however, no real attempt was made to compare the absolute intensities from the various alloys since it depends strongly on sample properties and thus becomes a very formidable task.

The A_6 spectra of a given composition were of course very similar to the A_5 spectra. However, the A_6 lines are less accurately determined since their intensities are always much less than the A_5 intensities over this range of composition. For the most favorable case used, $x = 0.181$, Eq. (1) gives $A_4 = 0.27$, $A_5 = 0.42$, $A_6 = 0.24$; thus we never get much A_6 intensity.

Fig. 3 shows a plot of the frequency of each spectral component as a function of composition. Table II gives a summary of the shifts due to putting the Nth *D*-type Fe atoms in the various shells. We see from Table II that the sixth Fe in the 1nn causes a shift of about 1 MHz, or 14% less than the fifth Fe did. In the 4nn shell each additional Fe atom added beyond the 13th causes a shift which is about 5% less than the previously added Fe atom. There is even a saturation or shielding between shells; i.e., the shift at an A_5-type Fe atom due to adding a 13th or 14th Fe atom in the 4nn shell is

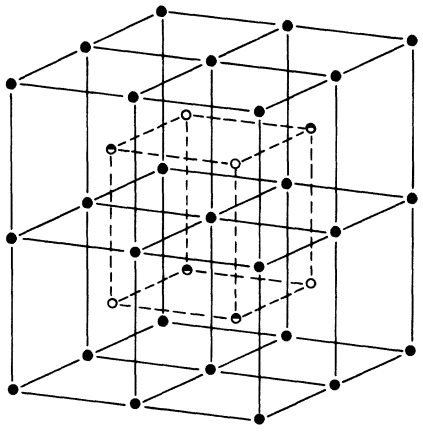

FIG. 1. Structure of ordered Fe_3Si.

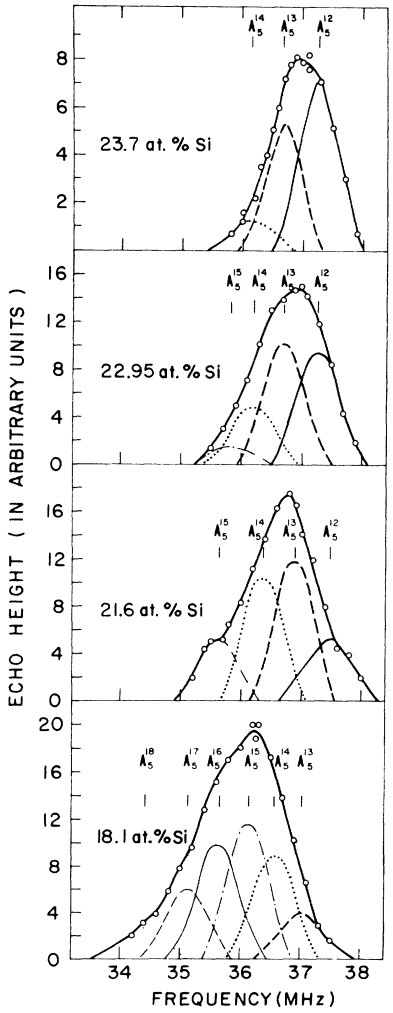

FIG. 2. Some typical A_5 spectra. The superscript denotes the number of Fe atoms in the 4nn shell. The curves are unfolded as discussed in the text. The pulse lengths were $\tau_1 \simeq 1\ \mu$sec, $\tau_2 \simeq 2.1\ \mu$sec and maximum turning angles were $\alpha_1 \simeq 5$ rad, $\alpha_2 \simeq 10.5$ rad.

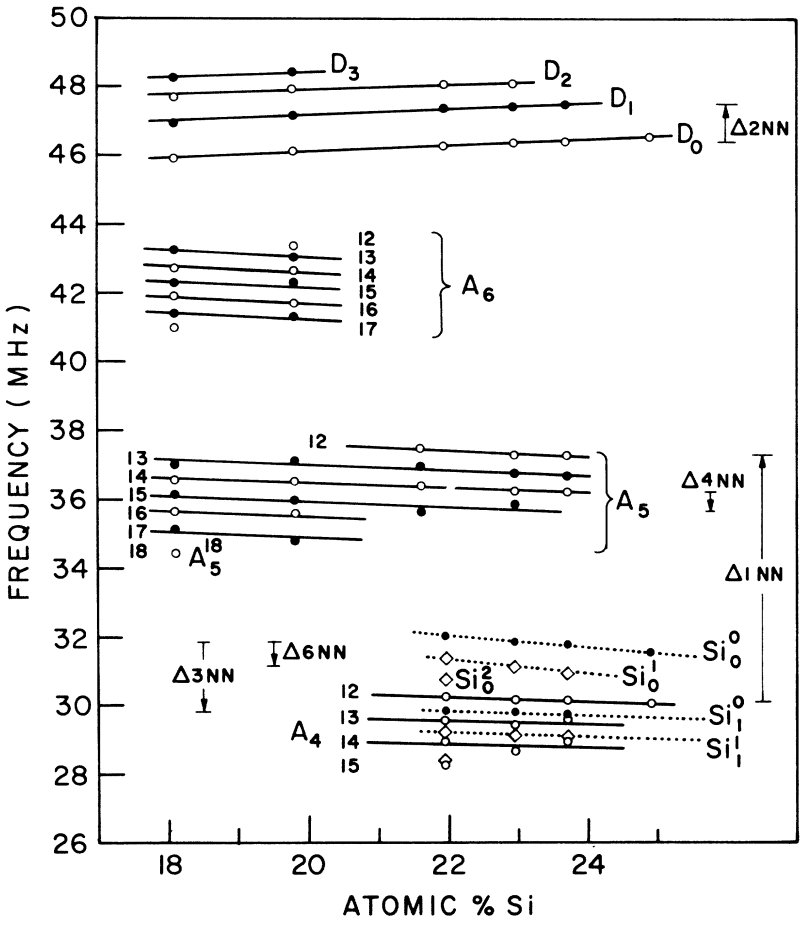

FIG. 3. Frequency variation of each occupational configuration as a function of percent Si in the alloys. See text for notation. The magnitude and direction of the frequency shifts caused by the various neighbor shells are indicated by the arrows.

-0.56 ± 0.03 MHz, which is about 14% less than the comparable shift, -0.65 ± 0.03 MHz for an A_4 atom, and an A_6-type Fe atom has about a 17% less shift than the A_5 type.

Note that the shift due to an added 4nn Fe atom decreases the frequency whereas an added 1nn Fe increases the frequency. Since the hyperfine field is negative an increase in frequency corresponds to a negative polarization. Thus the polarization due to an Fe atom in this lattice is negative at the 1nn distance and positive at the 4nn distance.

TABLE II. Shifts Δ_N for A sites due to the Nth D-type Fe atom in 1nn, 4nn, and 7nn shells (Δ_N in MHz).

Shell	Nth Fe atom			
1nn	5		6	
Δ_1	$+7.20 \pm 0.05$		$+6.19 \pm 0.02$	
4nn	13	14	15	16
$\Delta_4(A_4)$	-0.65 ± 0.03 (av. for 13, 14)			
$\Delta_4(A_5)$	-0.58 ± 0.02	-0.55 ± 0.04	-0.53 ± 0.10	-0.50 ± 0.05
		-0.54 ± 0.03 (av. for 13-17)		
$\Delta_4(A_6)$		-0.45 ± 0.05 (av. for 13-18)		
7nn				
Δ_7	$\simeq \lvert 0.2 \pm 0.4 \rvert$			

B. D Sites (2nn, 5nn)

From Table I we see that increasing the Fe content from stoichiometry adds Fe atoms into the 2nn, 5nn, and 8nn shells surrounding a D-type atom. We shall denote the D-type atoms by D_m, where here m gives the number of Fe atoms in the 2nn shell. The shift due to the 5nn atoms is so small that it is not resolvable but we can obtain an estimate of it from the broadening of the D_0 component in the spectra. For Fe_3Si, D_0 is a single sharp line at 46.53 ± 0.02 MHz. Fig. 4 shows some typical unfolded D spectra. Less-well-resolved spectra of these lines were published earlier[6]; however, there the dipolar structure of the D_m ($m \geq 1$) components was not taken into account and the fits obtained were not of the quality of those presented here. In Fig. 4 we see that there is clearly evidence of dipolar structure due to the Fe moments added in the second shell. This dipolar structure depends on the number of Fe's in the 2nn

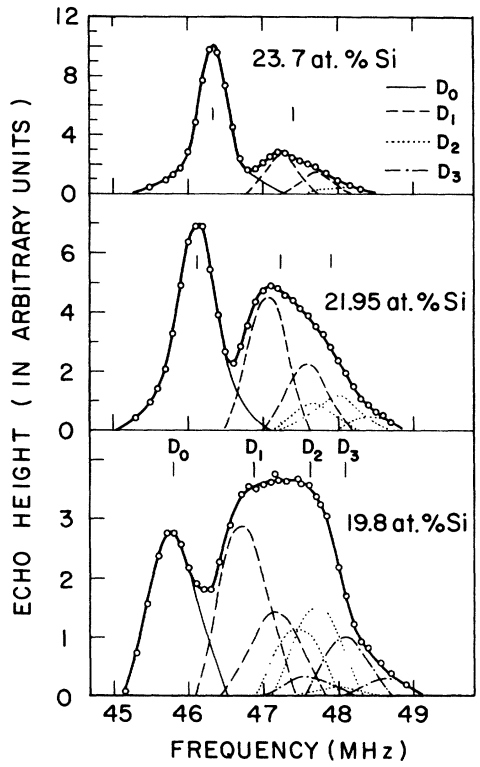

FIG. 4. Some typical D spectra. The subscript gives the number of Fe atoms in the 2nn shell. The structure in D_1, D_2, and D_3 is due to dipolar splitting as discussed in the text. The pulse lengths and turning angles were the same as for Fig. 2.

shell and is given by the usual dipolar shift formula $\gamma_{Fe}\mu(1-3\cos^2\theta)/r^3$, where θ is the angle between the direction of magnetization and the vector to the added Fe atom in the second shell ($\theta=0$ or $\frac{1}{2}\pi$), γ_{Fe} is the nuclear gyromagnetic ratio, and μ is the magnetic moment of the added D-type Fe atom. (There is no dipolar broadening for the 1nn shell since there $\cos\theta=\sqrt{3}/3$.) The estimated value of $\delta=\gamma_{Fe}\mu/r^3$ for the 2nn shell is $\simeq 0.14$ MHz, since $\mu\simeq 2.4\mu_B$[10] and $r\simeq 2.83$ Å.[11] In Fig. 4 we see that we can easily resolve the structure due to the dipolar field, in fact it must be considered to obtain good fits. The probability of having m Fe atoms in the 2nn shell for an alloy $Fe_{1-x}Si_x$ is given by

TABLE III. Shifts Δ_N for D sites due to Nth D-type Fe atom in the 2nn and 5nn shells (Δ_N in MHz).

Shell	N		
2nn	1	2	3
Δ_2	$+1.07\pm0.02$	$+0.70\pm0.03$	$+0.51\pm0.05$
δ	0.16 ± 0.01	0.11 ± 0.02	0.15 ± 0.04
% decrease		35%	30%
5nn			
Δ_5	-0.22 ± 0.05 (from broadening of D_0)		

$$P_m=\binom{6}{m}(1-4x)^{6-m}(4x)^m \quad . \tag{3}$$

The spectra were unfolded by starting from the left and stripping off each component such that the area of each component D_m corresponded to the fraction P_m while keeping the widths of all components essentially the same. The fits are excellent as seen in Fig. 4. In Table III the values for the hyperfine field shifts and dipolar splitting δ are listed for each Fe atom added to the 2nn shell. The values of δ obtained agree well, within the experimental uncertainties, with the estimated δ above. Again, we also see the saturation or shielding effect of Fe atoms. The percent decrease in the shift is also listed for each Nth Fe atom added. It is especially large for the 2nn shell, being about 30% for the second and third Fe atoms added to the shell.

We can obtain an upper limit to the shift due to the 5nn shell from the broadening of the D_0 component. This is a rather accurate determination since, as seen in Fig. 4, the D_0 line is quite well resolved. The upper part of Fig 5 shows the broadening, with respect to the 24.0-at.% alloy, of D_0 as a function of composition for the alloys of 19.8-at.% Si and greater. Assuming a Gaussian line

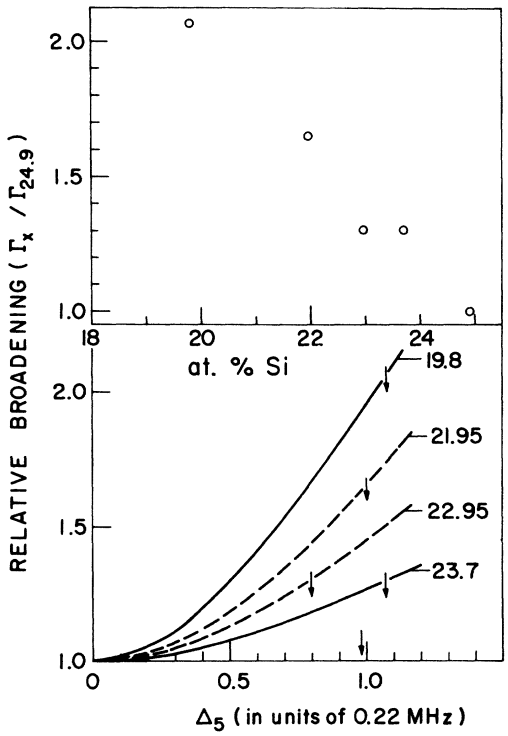

FIG. 5. The upper half shows the broadening of the D line of the alloy $Fe_{1-x}Si_x$ relative to D_0 in the 24.9-at.% Si alloy. The lower portion gives the calculated broadening of a Gaussian-shaped line due to a shift Δ_5 (in units of the half-width at the $1/e$ height) per Fe atom in the 5nn shell. The arrows show the experimentally observed broadenings.

shape we then calculate on a computer the broadening for each alloy due to a shift Δ_5, (in units of the half-width at the $1/e$ height, 0.22 MHz for the 24.9-at.% Si), for each Fe added in the 5nn shell. This neglects any saturation effects, which is probably safe for the 5nn shell especially since the 1nn shell is completely full of Fe atoms. The saturation effect per Fe atom for the 4nn shell when the number of Fe's in the 1nn shell was constant was seen to be only about 5% per added Fe. The lower part of Fig. 5 shows the calculated broadening as a function of Δ_5. The observed broadening for each alloy is shown by the arrows. The observed broadening thus corresponds to a Δ_5 of about 0.98 ± 0.05. We now suggest that the observed shift is essentially due entirely to the 5nn shell and that it decreases the frequency of D_0 for the following reasons: (i) To anticipate the final result, the next shell having an influence on the D sites, the 8nn shell, appears to be near a node. The next shell after that which gets added Fe atoms in the 13nn shell whose effect should be negligible. (ii) In Fig. 3 we see that the slopes of the D_n frequency lies are positive whereas those for Si and A_m^n sites are negative. We can understand part of the negative value in terms of the lattice parameter change with alloying as discussed in Sec. IV E. However, we would like to minimize the difference in the slopes of the A and D frequency lines. Accompanied by the broadening discussed above is also a shift of center of the line. It is therefore most likely that the shift due to the 5nn shell is in the direction to make the slopes of the D_m lines more negative. A negative value of Δ_5 is in the correct direction. The frequency values shown plotted in Fig. 3 thus contain this assumption that Δ_5 decreases the frequency. The corrections to the position of the D_0 line are small, the largest being only 0.4 MHz for the 18.1-at.% Si alloy. We thus assume that broadening of the D_0 lines is due to the 5nn shell which produces a negative frequency shift. This corresponds to a positive polarization which seems reasonable in comparison with both the magnitude and sign of the 4nn shift.

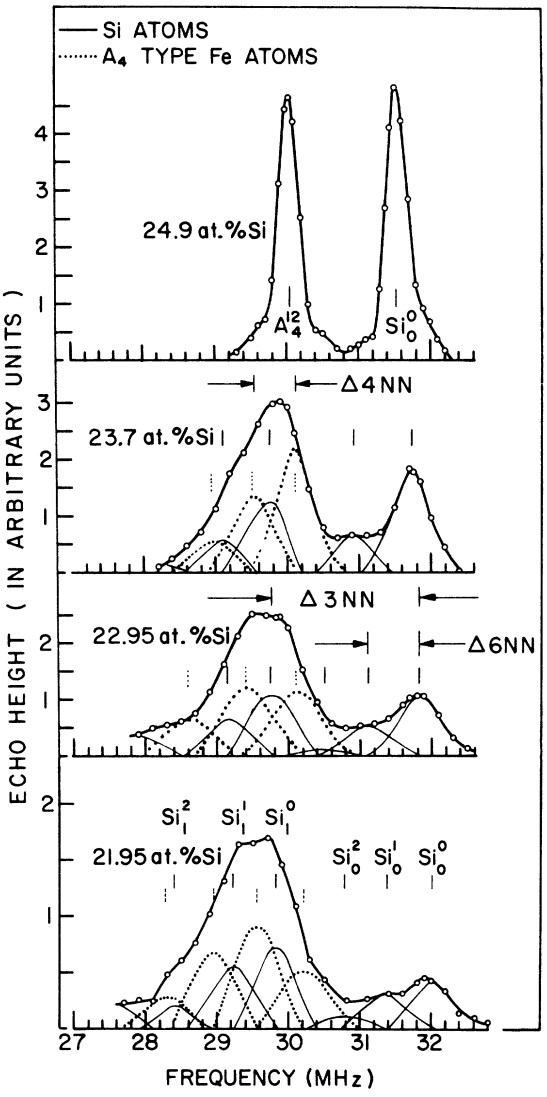

FIG. 6. Some typical Si and A_4 spectra for various composition alloys. For Si sites the subscript gives the number of Fe atoms in the 3nn shell and the superscript the number of Fe atoms in the 6nn shell. The pulse lengths and turning angles were the same as for Fig. 2.

C. Si Sites (3nn, 6nn, 9nn)

From Table I we see that the Si sites are sensitive to the 3nn, 6nn, and 9nn. We shall denote the Si atoms by Si_m^n, where m gives the number of D-like Fe atoms in the 3nn shell and n the number of Fe atoms in the 6nn shell. Fe_3Si shows a single sharp line for the Si atoms at 31.53 ± 0.02 MHz, corresponding to an internal field of 37.2 kG; typical spectra are shown in Fig. 6. The bumps in the wings of the Si_0^0 and A_4^{12} spectra of 24.9-at.% Si are due to frequency sidebands as discussed in Ref. 9. The spectra for alloys of lower Si content show a definite contribution near 31 MHz which, from its intensity, is easily identified as due to the 6nn shell. Since the 3nn shell has twice as many atoms as the 6nn shell, Si_1^0 has about twice the intensity of Si_0^1 in this alloy range. The shifts due to Fe atoms in the 3nn and 6nn shells both decrease the frequency, and so the Si spectra of the alloys off stoichiometry overlap with the A_4 spectra. However, from the A_5 spectra we have confidence that we know the shape of the A_4 spectra very well so we are able to unfold the low content Si spectra very reliably as shown in Fig. 6. The dipolar shift δ for the 3nn shell should be about 0.05 MHz.

TABLE IV. Shifts Δ_N for Si sites due to D-type Fe atoms in 3nn, 6nn, and 9nn shells (Δ_N in MHz).

Shell	For Si	For Fe	
3nn	-2.08 ± 0.05	-1.35 ± 0.03	(for 1-3nn)
Δ_3	$-2.0\ \pm0.1$	$-1.3\ \pm0.06$	(for 2-3nn)
6nn	-0.72 ± 0.05	-0.47 ± 0.04	(for 0-3nn, 1-6nn)
Δ_6	-0.61 ± 0.03	-0.40 ± 0.02	(for 1-3nn, 1-6nn)
9nn	$\simeq\lvert0.16\pm0.02\rvert$	$\simeq\lvert0.10\pm0.01\rvert$	(from broadening of Si_0^0)

It may cause the asymmetry in the Si_1^0 component of the 23.7-at.% Si alloy; the magnitude and direction are correct (see Fig. 6). Otherwise it was not discernible. We unfold by stripping from the right using the calculated areas and a constant width for each Si component of a given alloy, as discussed before. The broadening of the well-resolved Si_0^0 component (see Fig. 6) was used to obtain an upper limit to the shift per Fe atom in the 9nn shell. The manner of determination was similar to that used to obtain the 5nn shift as discussed in Sec. III B on D sites.

Table IV gives the measured shifts for the different shells and the frequency values are shown in Fig. 3. We again see an intershell saturation effect, i.e., the shift due to an Fe in the 6nn shell is smaller when there is an Fe in the 3nn shell than when there is not. There also seems to be a slight intrashell shielding in the 3nn shell although it is much smaller than that observed for the 1nn and 2nn shells. Column 2 gives the shift in frequency as seen by the Si nuclei. We convert this to the equivalent hyperfine field at an Fe nucleus by using the hyperfine structure constants. Values for the hyperfine fields at a nucleus due to one ns electron have been given and discussed by Shirley and Westenbarger[12(a)] and by Kopfermann.[12(b)] We use extrapolated values which agree with these works. As pointed out in Ref. 12(b), the agreement is quite good. It is difficult to assign an error to the accuracy of the hyperfine-field constants for elements other than those discussed in Ref. 12(b) (which have essentially no error). We use for Si, $H_{3s}^{Si}=0.50$ MG and for Fe, $H_{4s}^{Fe}=2.0$ MG. [The Al value of Ref. 12 (0.49 MG) is consistent with the measured hyperfine field of -55 kG[13] observed for dilute Al in an Fe matrix. Assuming the field at an Al atom is entirely due to conduction-electron polarization (CEP) from all its Fe neighbors, we would obtain ~-50 kG.] We make the reasonable assumption that the s-conduction electrons take on the wave function character of the s valence electrons characteristic of an atom when in the vicinity of its nucleus. Thus if we had a polarization p of the s-conduction electrons, the field at the Si nucleus would be pH_{3s}^{Si}, corresponding to a frequency $\nu_{Si}=\gamma_{Si}pH_{3s}^{Si}$. Similarily, at an Fe nucleus we would observe $\nu_{Fe}=\gamma_{Fe}pH_{4s}^{Fe}$. Thus $\nu_{Fe}=\gamma_{Fe}H_{4s}^{Fe}\nu_{Si}/\gamma_{Si}H_{3s}^{Si}=0.65\nu_{Si}$. The corresponding frequency shifts at an Fe nucleus are listed in column 3 of Table IV.

D. Relative Intensities of Si_0^0 and A_4^{12}

The relative areas of the A_4^{12} and Si_0^0 lines for Fe_3Si are nearly equal, as seen in Fig. 6. We show that this agrees excellently with value expected from the measured enhancement factors. The emf induced in a coil of area A by the precessing nuclear magnetization is $\mathcal{E}=4\pi\omega_0MA$, where M is the nuclear magnetization of the sample given by $M=\chi H_{int}=N\gamma^2\hbar^2I(I+1)H_{int}/3kT$. ω_0 is the resonance frequency and N is the number of nuclei with spin. However, we do not observe the nuclear magnetization but the electronic magnetization produced by the coupling between the nuclei and electrons through the enhancement factor. The simulated-echo procedure eliminates one frequency factor; thus the ratios of the observed voltages for the A_4 and Si lines in Fe_3Si are given by

$$\frac{V_{Si}}{V_{A4}}=\frac{N_{Si}\gamma_{Si}\nu_{Si}\epsilon_{Si}}{N_{A_4}\gamma_{Fe}\nu_{A_4}\epsilon_{A_4}}=6.7\,\frac{\epsilon_{Si}}{\epsilon_{A_4}}=1.02\pm0.03\,, \qquad (4)$$

since the measured value of $\epsilon_{A_4}/\epsilon_{Si}=6.6\pm0.2$. The ratio of the measured areas of the Si and A_4 lines is 1.03.

E. General Considerations

In order to express the shifts in terms of percentage shifts for a pure Fe-like lattice we extrapolate from a D_0-Fe atom in Fe_3Si to the field H_{Fe}' which would be expected for an Fe atom entirely surrounded by other Fe atoms. In Fig. 7 we show the extrapolation used for the 2nn shifts. We use -0.15 MHz as an average value for the 5nn. We assume the effects of higher shells (i.e., 8nn and 13nn) are negligible (see Fig. 8). We get H_{Fe}'

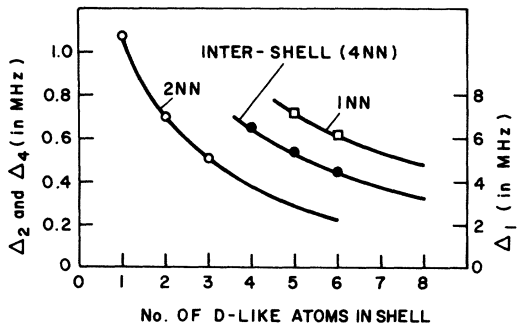

FIG. 7. Saturation or shielding effects for various shells. The curves labeled 1nn and 2nn are due to intrashell saturation. The curve marked intershell gives the nn shifts for different numbers of Fe atoms in the 1nn shell.

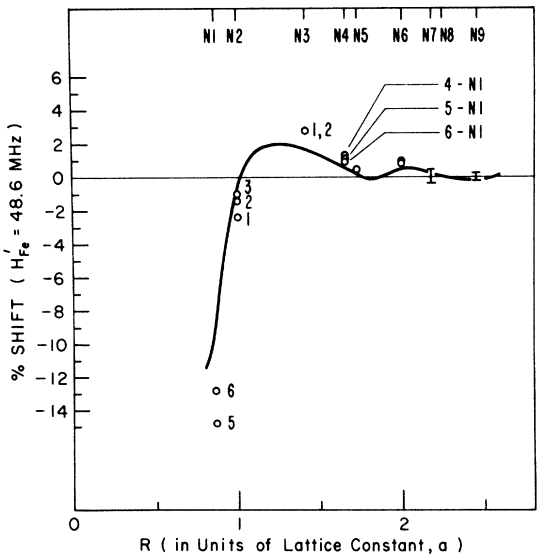

FIG. 8. Percentage shifts per D-like Fe atom in the first 9nn shells. The number beside the data points indicates which Fe atom in the shell is causing the shift as explained in the text. The solid line corresponds to the estimated shift caused by the last atom in a full shell, as would be obtained in dilute alloys. The value at the origin is estimated in Paper II in the text to be about +60%.

= 48.5 MHz from D_0 type atoms. We apply a similar procedure to the A-type atoms. In Fig. 7 the curve marked 1nn shows the measured and extrapolated values used for the 1nn shell. We also show the measured and extrapolated intershell values of the 4nn shift due to adding the 13–15 D-type Fe atoms into the 4nn shell, for various numbers of Fe atoms in the 1nn shell. The intershell saturation due to 1nn is seen to be much larger than the 4nn intrashell shielding (see Table II). We use − 0.3 MHz for the 4nn shift and − 0.1 MHz for the 7nn shift. We assume the effects of the 10nn, 12nn, and higher shells cancel out and obtain H'_{Fe} = 48.8 MHz. We shall use H'_{Fe} = 48.6 MHz to obtain the percentage shifts. Table V gives the percentage shifts through the 9nn shell. We have plotted these values in Fig. 8, where the number beside the data points indicates which Fe atom in that shell is causing the shift. For Δ_4 it indicates the number of Fe atoms in the 1nn shell. Since the hyperfine field is negative an increase in frequency means a negative shift. The solid curve is the estimated extrapolated value of the shift caused by the last Fe in a full shell; that is, it should be closely related to the shift measured in a dilute alloy.

IV. DISCUSSION OF EXPERIMENTAL RESULTS

We shall interpret the internal field shifts as due to CEP effects of the 4s-like conduction electrons. We want to emphasize that this type of analysis should only apply to alloy systems where the solute atom has no moment and the form factor of the Fe atoms does not change upon alloying. As more fully discussed in Ref. 2(b) these conditions are known to be true for dilute Al and Si alloys[14,15] of Fe and also hold fairly well in the ordered Fe_3Si and Fe_3Al alloys.[16] If the solute atom has a moment or the Fe moment distribution changes very much, it becomes very difficult to separate the effects of changes in core polarization from CEP effects.

The "dilute alloy" curve of Fig. 8 has a very similar behavior to that measured for dilute FeSi alloys.[2,4] We will therefore now combine the two measured curves to try to obtain a best curve for the CEP surrounding an Fe atom in a pure Fe lattice. In Table VI we list the extrapolated shifts from this experiment, the data from the dilute alloy Mössbauer[2(c),2(d)] measurements, and the best average NMR data from Ref. 4 and more recent unpublished measurements. No value is listed in Column 2 for $N1$, because part of the shift measured as Δ_1 in the ordered alloys is undoubtedly due to a change in moment of the A-type atoms as Fe is added in the 1nn shell. Since we do not know how the A atom moment changes with the number of 1nn Fe atoms, it is difficult to evaluate this contribution. This difficulty does not arise for any of the other shells since the moment change of the D and Si atoms upon adding Fe is negligible and the 4nn and 7nn shifts are obtained from a given A_m configuration so there is no moment change. On the other hand, the value of Δ_1 obtained from the dilute alloys is very accurately determined and thus we list this as the pure Fe value in column 5. The Δ_2 value obtained in these measurements may be lower than that obtained in the dilute alloys because as seen in Table I the D-type atoms have all A-type atoms in the 1nn shell. These A-type atoms probably do not shield as well as Fe atoms in an Fe lattice (which are very close to D-type atoms). Thus the shielding or saturation effects observed here for the 2nn shell may indeed be larger than would exist in pure Fe and thus yield too small a value for Δ_2. We therefore tend to favor the dilute alloys value for this case. The Δ_3 values are seen to be very close for all three experiments. The Δ_4 and higher percentage shifts are much more accurately obtained in this experiment so we weight them heavily in obtaining the pure Fe values given in Column 5. These are shown plotted in Fig. 9. Using the hyperfine coupling constant H_{4s}^{Fe} = 2.0 MG, we can calculate the polarization p_N at a given shell distance from an Fe atom by $p_N = \Delta_N H_{Fe}/(nH_{4s}^{Fe})$, where n is the number of conduction electrons per Fe atom. The right-hand scale in Fig. 9 corresponds to the values of p_n calculated with n = 0.8.

TABLE V. Percentage shifts caused by an Nth D-type Fe atom in the various shells (H^{t}_{Fe} = 48.6 MHz).

Δ_1					5-1nn -14.8 ± 0.1		6-1nn -12.8 ± 0.04
	1-2nn	2-2nn	3-2nn				
Δ_2	-2.20 ± 0.04	-1.44 ± 0.06	-1.05 ± 0.1				
	1-3nn	2-3nn					
Δ_3	$+2.8\pm0.1$	$+2.7\pm0.1$					
				4-1nn (13-14)-4nn $+1.33\pm0.06$			
Δ_4					5-1nn		
				13-4nn $+1.19\pm0.04$	14-4nn 1.13 ± 0.08	15-4nn 1.09 ± 0.2	16-4nn 1.03 ± 0.1
							6-1nn (13-18)-4nn 0.92 ± 0.1
Δ_5		$+0.45\pm0.1$ (from broadening of D_0)					
	0-3nn, 1-6nn						
Δ_6	$+1.0\pm0.1$						
	1-3nn, 1-6nn						
	$+0.8\pm0.1$						
Δ_7		$\leq\lvert0.4\pm0.08\rvert$					
Δ_9		$\leq\lvert0.2\pm0.03\rvert$					

Using the values in column 2 Table VI we estimate the frequency of the Si atom in Fe_3Si assuming that the field is entirely due to the CEP from the Fe neighbors. Considering whether the shells contain A- or D-type Fe atoms and assuming that the CEP is proportional to the moment we obtain $\nu_{Si} = -25$ MHz (the negative sign indicates the field is opposite to the magnetization). This is in reasonable agreement with the observed frequency of 31.5 MHz.

A. Isotropy of Fermi Surface of 4s-like Electrons

We see in Figs. 8 and 9 that all the experimental points appear to lie on a smooth curve. Since these points represent many different crystallographic directions, the smoothness indicates that the value of the Fermi wave vector, k_F, is nearly the same

TABLE VI. Values used for derivation of pure Fe percentage shifts for various neighbor shells from FeSi alloys.

		Experiment Dilute alloys		Best Fe value
Shell	Fe_3Si	NMR	Mössbauer	% Shift
Δ_1		-8.0	-8.0	-8.0
Δ_2	-0.6	-1.8	-3.0	-1.8
Δ_3	$+1.7$	$+1.5$	$+1.6$	$+1.6$
Δ_4	$+0.6$		0.0 ± 0.5	$+0.4$
Δ_5	$+0.3$		-0.3 ± 0.3	$+0.2$
Δ_6	$+0.5$		$+0.2\pm0.3$	$+0.4$
Δ_7	$\leq\lvert0.4\rvert$		(probably close to $+0.3$)	
Δ_9	$\leq\lvert0.2\rvert$		(probably close to -0.2)	

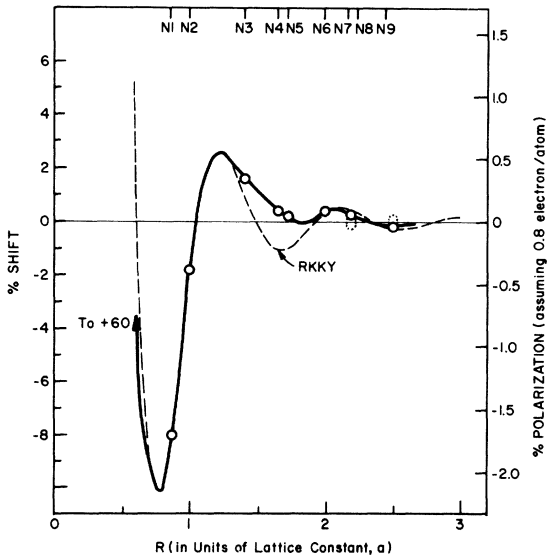

FIG. 9. Extrapolated percent hyperfine field shifts for each neighbor shell in pure Fe as a function of the distance of that shell from the origin (solid curve). These shifts are interpreted to be a measure of the variation of the spin polarization of the 4s-like electrons with distance from a Fe atom. The dashed curve shows the RKKY approximation for $k_f = 1.28\times10^8$ cm^{-1} and $J_{int}(q=0) = 0.9$ eV (see Paper II).

in these directions and that thus the Fermi surface is quite isotropic. Δ_1 and Δ_5 are in the same direction (111), as are Δ_2 and Δ_6 (100). No $4s$-like Fermi surfaces have been obtained in the latest band structure calculations,[8] in fact the meaning and determination of the $4s$-like Fermi surface in the hybridized region is obscure, but it would be of interest to investigate this problem further.

B. Dipolar Effects

We clearly observed dipolar effects in the 2nn shell which were in excellent agreement with the estimated value, see Table III. Cranshaw *et al.*[17] interpreted the results of a clever Mössbauer experiment on an $Fe_{0.94}Si_{0.06}$ alloy as due to a large pseudodipolar moment of $-8.0\mu_B$ at second neighbors arising from the asphericity of the spin density caused by an impurity atom. Since we observe a dipolar structure which corresponds excellently to that expected from an added Fe moment of the D-type atoms in a 2nn shell, we conclude in disagreement with Cranshaw *et al.* that the pseudodipolar effects are negligible in these alloys and, since the situation is analogous, also probably in the dilute alloys. We know that the dilute Si alloys strongly tend to order; this may have given some difficulty in the experiments of Cranshaw *et al.*

C. Saturation or Shielding Effects

We have seen from Tables II–IV and Fig. 7 that there are definite and strong shielding effects of one Fe atom by another. Both intrashell and intershell shielding effects were observed to be present. This indicates that the linear approximation usually used in deriving spin density effects is not valid. From Fig. 7 we see that the shielding effects become smaller as the shell is filled. For the 1nn shell we estimate that there should be about a 12% greater shift due to a second atom being removed from the shell as compared with the shift of the first. In the 2nn shell this is increased to about a 25% greater effect. The 2nn shell having a greater shift is not unreasonable since we might expect the shielding effects to be greater the fewer atoms there are in a shell. However, as mentioned earlier the 2nn shielding may be exaggerated in these ordered alloys, since the D-type Fe atoms have A Fe atoms in their 1nn shell and thus perhaps less shielding by 1nn than in pure Fe. A saturation effect was first measured in the Mössbauer experiment of $Fe_{0.94}Si_{0.06}$ by Cranshaw *et al.*[17] They observed about 30% greater shift for the second atom than for the first atom removed from the 1nn shell. This is about twice as large as the effect observed here for going from six to five atoms in the 1nn shell, and about three times as large as the value we extrapolate for removing the second atom. The discrepancy may be attributable to the lesser accuracy of the Mössbauer technique or also to the fact that dilute FeSi alloys do not completely disorder.[2(d)] The analysis of line shapes from dilute-alloy NMR or Mössbauer experiments usually neglects saturation and assumes additivity of the effects of atoms in the various shells. While we see that this leads to some error it is probably the only practical approach in order to keep the number of parameters to a reasonable level.

D. Another Nonlinear Effect: Damping of RKKY Oscillation

A second kind of predicted nonlinear effect is due to the impurity sites introducing nonperiodicity in the lattice and thus a spread in k values for the simple Bloch wave characteristic of the perfect lattice.[7] DeGennes showed that this introduces a phase shift and damping factor of the RKKY oscillations. The damping factor goes as $e^{-r/\lambda}$, where λ is the mean free path of the conduction electrons which is inversely proportional to the impurity concentration. Neglecting the phase shift we would expect to see the Δ_N's decrease as $\Delta_N{}^{-r/\lambda}$ as we decrease the Si content. For example, we would expect the A_5 lines in Fig. 3 to converge as we go to smaller Si content. Note that this effect is clearly separable from saturation effects which change the spacing between the configuration lines in Fig. 3, but keeps them parallel. No converging effect is discernible in the data. Here the most sensitive shift to observe such a damping is Δ_4 of the A_5 spectra. From the observed Δ_4 values we can estimate a lower limit to the mean free path such that no damping effect would be observed here. We estimate that at most the decrease in Δ_4 might be about 8%. From this we estimate a lower limit for λ of about 120 lattice constants per at.% Si. This value agrees well with the value of ~130 lattice constants per at.% Si estimated using a free-electron-gas model: $\lambda(\text{Å}) = 4.7\times10^3/\rho_0 E_F$, where ρ_0 is the residual resistivity in $\mu\Omega$ cm/at.% taken as 7 $\mu\Omega$ cm/at.% Si,[18] and E_F is the Fermi energy in eV, ~5eV from the Fe band calculation.[8]

E. Variation of Frequencies with Alloying: Volume Dependence of the Hyperfine Field

There is a further separate effect evident in the data which is manifest in Fig. 3 by the slope in the lines; that is, the change in frequency of a given type configuration with alloying. This effect is different from the saturation or shielding effect of one Fe atom by another in the same alloy, which was discussed in Sec. IV C. The saturation effect is manifest in Fig. 7 by the *change* in spacing between the lines for a given type site; e.g., the difference in spacing between $D_0 - D_1$ and $D_1 - D_2$ lines, etc., due to different numbers of 2nn's around D-type atoms (in the same alloy). The change in frequency of a given configuration with alloying is

believed to be related to the volume change upon alloying. In correlating these frequency changes to the volume (or pressure) changes we find that a much more complex treatment than that existing in the literature is necessary. To make this analysis, a definite hyperfine field model is required, so this effect is discussed in Sec. VI of Paper II rather than here.

V. CONCLUSIONS

The hyperfine field shifts of different type sites in the ordered FeSi alloys have been measured and combined with dilute FeSi alloy data to give the 4*s*-like CEP distribution as a function of distance around each Fe atom in a pure Fe lattice. The smoothness of this distribution indicates that the Fermi surface of the 4*s*-like electrons is fairly isotropic. Dipolar and saturation or shielding effects were clearly seen; the dipolar effects were of the magnitude expected with no pseudodipolar effects. A lower limit of the mean free path of the conduction electron in these alloys was obtained from the lack of a damping effect of the RKKY oscillations. It agrees well with that obtained from resistivity measurements on these alloys.

Using the CEP data obtained here and the latest Fe band calculations we are able to obtain a consistent model for the origin of the hyperfine field in pure Fe and at solute atoms in dilute alloys of Fe. This is presented in the following paper.

---

[1]C. Zener, Phys. Rev. 83, 299 (1951); M. A. Ruderman and C. Kittel, *ibid.* 96, 99 (1954); T. Kasuya, Progr. Theoret. Phys. (Kyoto) 16, 45 (1956); K. Yosida, Phys. Rev. 106, 893 (1957).

[2](a) M. B. Stearns, Phys. Rev. 129, 1136 (1963); J. Appl. Phys. 35, 1095 (1964); (b) M. B. Stearns and S. S. Wilson, Phys. Rev. Letters 13, 313 (1964); (c) M. B. Stearns, J. Appl. Phys. 36, 913 (1965); (d) 147, 439 (1966).

[3]G. K. Wertheim, V. Jacarrino, J. H. Wernick, and D. N. E. Buchanan, Phys. Rev. Letters 12, 24 (1964).

[4]M. Rubinstein, G. H. Stauss, and M. B. Stearns, J. Appl. Phys. 37, 1334 (1966).

[5]J. I. Budnick, S. Skalski, and T. J. Burch, J. Appl. Phys. 38, 1137 (1967); J. J. Murphy, J. I. Budnick, and S. Skalski, *ibid.* 39, 1239 (1968).

[6]M. B. Stearns, L. A. Feldkamp, and J. F. Ullrich, Phys. Rev. Letters 30A, 443 (1969).

[7]P. G. de Gennes, J. Phys. Radium 23, 630 (1962).

[8](a) K. J. Duff and T. P. Das, Phys. Rev. B 3, 192 (1971); (b) 3, 2294 (1971).

[9]M. B. Stearns, Phys. Rev. 162, 496 (1967).

[10]A. Paoletti and L. Passari, Nuovo Cimento 32, 25 (1964).

[11]W. B. Pierson, *A Handbook of Lattice Spacings* (Pergamon, New York, 1958).

[12](a) D. A. Shirley and G. A. Westerbarger, Phys. Rev. 138, A170 (1965); (b) also see H. Kopfermann, *Nuclear Moments* (Academic, New York, 1958), who in particular compares experimental and calculated hyperfine field values for several elements.

[13]M. Kontani and J. Itoh, J. Phys. Soc. Japan 22, 345 (1967).

[14]M. Fallot, Ann. Phys. (Paris) 6, 305 (1936); A. Arrott and H. Sato, Phys. Rev. 114, 1420 (1959).

[15]A. Arrott, M. F. Collins, T. M. Holden, G. G. Low, and R. Nathans, J. Appl. Phys. Suppl. 37, 1194 (1966).

[16]R. Nathans, M. T. Pigott, and C. G. Shull, J. Phys. Chem. Solids 6, 38 (1958).

[17]T. E. Cranshaw, C. E. Johnson, and M. S. Ridout, *Proceedings of the International Conference on Magnetism, Nottingham*, 1964 (The Institute of Physics and the Physical Society, London, 1965), p. 141.

[18]M. G. Corson, Trans. AIME 80, 249 (1928); F. W. Glaser and W. Ivanick, *ibid.* 106, 1290 (1956).